Cellular Physiology and Biochemistry

Cell Physiol Biochem 2013;32:11-24
DOI: 10.1159/000350119
Published online: July 04, 2013
Accepted: June 14, 2013

1421-9778/13/0321-0011$38.00/0

Original Paper

Investigation of the Inhibitory Effects of the Benzodiazepine Derivative, 5-BDBD on $P2X_4$ Purinergic Receptors by two Complementary Methods

Bernadett Balázs[a] Tamás Dankó[a] Gergely Kovács[b,c] László Köles[d] Matthias A. Hediger[b,c] Ákos Zsembery[a]

[a]Institute of Human Physiology and Clinical Experimental Research, Semmelweis University, Budapest; [b]Institute of Biochemistry and Molecular Medicine, University of Bern; [c]Swiss National Centre of Competence in Research, NCCR TransCure, University of Bern; [d]Department of Pharmacology and Pharmacotherapy, Semmelweis University, Budapest

Key Words
Calcium influx • Electrophysiology • ATP • 5-BDBD • P2X receptors

Abstract
Background/Aims: ATP-gated $P2X_4$ purinergic receptors ($P2X_4Rs$) are cation channels with important roles in diverse cell types. To date, lack of specific inhibitors has hampered investigations on $P2X_4Rs$. Recently, the benzodiazepine derivative, 5-BDBD has been proposed to selectively inhibit $P2X_4Rs$. However, limited evidences are currently available on its inhibitory properties. Thus, we aimed to characterize the inhibitory effects of 5-BDBD on recombinant human $P2X_4Rs$. ***Methods:*** We investigated ATP-induced intracellular Ca^{2+} signals and whole cell ion currents in HEK 293 cells that were either transiently or stably transfected with $hP2X_4Rs$. ***Results:*** Our data show that ATP (< 1 μM) stimulates $P2X_4R$-mediated Ca^{2+} influx while endogenously expressed P2Y receptors are not activated to any significant extent. Both 5-BDBD and TNP-ATP inhibit ATP-induced Ca^{2+} signals and inward ion currents in a concentration-dependent manner. Application of two different concentrations of 5-BDBD causes a rightward shift in ATP dose-response curve. Since the magnitude of maximal stimulation does not change, these data suggest that 5-BDBD may competitively inhibit the $P2X_4Rs$. ***Conclusions:*** Our results demonstrate that application of submicromolar ATP concentrations allows reliable assessment of recombinant P2XR functions in HEK 293 cells. Furthermore, 5-BDBD and TNP-ATP have similar inhibitory potencies on the $P2X_4Rs$ although their mechanisms of actions are different.

Ákos Zsembery MD, PhD

Institute of Human Physiology and Clinical Experimental Research,
Semmelweis University Budapest, Tűzoltó utca 37-47, Budapest (Hungary)
Tel. +36206660339, Fax +3613343162, E-Mail zsembery.akos@med.semmelweis-univ.hu

Introduction

Extracellular ATP and its breakdown products regulate a number of cellular functions by stimulating purinergic receptors [1]. In the last two decades 19 different purinergic receptors have been identified including four adenosine-activated P1 receptors, seven ATP-gated P2X receptor (P2XR) channels and eight metabotropic P2Y receptors which can be stimulated by adenosine and uridine tri- and diphosphates [2].

The seven P2X receptor subunits ($P2X_{1-7}$) are widely distributed in both excitable and non-excitable cells providing cation permeable pathways (mainly for Ca^{2+} and Na^+) through the plasma membrane. Previous studies revealed that these subunits might assemble as either homo- or heterotrimeric receptors [2]. Importantly, heteromerization can change functional and pharmacological properties of the P2XRs [2]. P2XRs are involved in presynaptic and postsynaptic actions of ATP [3-5] including taste sensation [6], hearing [7] and chemoreception [8]. P2XRs are also necessary for proper function of immune system [9]. In cardiovascular, respiratory, genitourinary and gastrointestinal systems several P2X receptor subunits seem to play pivotal role in both endothelial and epithelial cell functions [10]. Using pharmacological approaches and knockout animals, it has also become evident that P2XRs are involved in a broad range of pathophysiological processes such as chronic and inflammatory pain [11-15] arthritis [16] male infertility [17] and hypertension [18, 19].

A role for $P2X_4$ receptors has been proposed in neuropathic pain [15], endothelial NO production [18], regulation of airway ciliary epithelia [20] and chloride secretion of respiratory [21, 22] and biliary epithelia [23]. However, validation of $P2X_4R$ involvement has been often hampered by the lack of specific inhibitors. In fact, $P2X_4$ receptors are insensitive to the nonselective inhibitors, such as suramin and PPADS [24]. TNP-ATP has been found as a putative antagonist of $P2X_4$ receptors. However, it blocks other P2X subtypes as well, such as $P2X_1$, $P2X_2$ and $P2X_3$ [25]. Furthermore, TNP-ATP has been shown to be a weak blocker of $P2X_4$ receptors (IC_{50} = 15 μM for 10 μM ATP stimulation) compared to its inhibitory potency at $P2X_1$ and $P2X_3$ receptors [26].

The benzodiazepine derivative, 5-(3-bromophenyl)-1,3-dihydro-2H-benzofuro[3,2-e]-1,4-diazepin-2-one (5-BDBD), has been recently shown to selectively inhibit $P2X_4$ receptors (IC_{50} ~ 0.5 μM) [27]. Nonetheless, these results are described in a patent and details of the experimental procedure are not available. So far, limited experience has been available with 5-BDBD and there is no consensus about its pharmacologically relevant concentration range. In some studies low micromolar (5-10 μM) concentrations were used [28, 29] whereas others applied significantly higher doses of 5-BDBD (30-100 μM) [30, 31].

In the present study, we investigated ATP-induced cytosolic Ca^{2+} signals and inward ion currents in HEK 293 cells transfected either transiently or stably with $hP2X_4$ receptors. We characterized $P2X_4$ receptor-mediated whole cell ion currents and identified P2YR- and P2XR-dependent calcium signals using electrophysiological and fluorescence ion measurement techniques, respectively. Despite endogenous expression of P2YRs we were able to discern P2XR-dependent Ca^{2+} signals stimulating the cells with submicromolar concentrations of ATP. We also assessed the inhibitory effects of 5-BDBD and TNP-ATP on both intracellular Ca^{2+} signals and inward ion currents. Our data suggest that 5-BDBD and TNP-ATP have similar inhibitory potencies on $P2X_4$Rs. Furthermore, we show that 5-BDBD functions as a competitive antagonist of $hP2X_4$Rs.

Materials and Methods

Materials

Cell culture medium, fetal bovine serum, cell culture supplements and antibiotics were purchased from Csertex Inc. (Budapest, Hungary). TurboFect™ *in vitro* Transfection Reagent was purchased from Biocenter (Szeged, Hungary). Lipofectamine 2000 was obtained from Invitrogen (Life Technologies Europe B.V, Zug, Switzerland). Fluo-3/AM was purchased from Invitrogen Inc. (Carlsbad, CA). 5-BDBD was obtained

from Tocris Inc. (Minneapolis, USA). Calcium-5 was purchased from Molecular Devices (Molecular Devices LLC, Sunnyvale, CA, USA). Ivermectin (IVM) was obtained from Merck AG (Merck, Zug, Switzerland). All other chemicals were purchased from Sigma-Chemical (St. Louis, MO).

DNA Construct

The human $P2X_4R$ (imaGenes GmbH, Berlin, Germany) was amplified from human cDNA with the following primer pair: 5'-TAT AAG ATC TCG CGG CCA TGG CGG GC-3',

5'-TAT AGA ATT CCC TGG TCC AGC TCA CTA GCA AGA CCC TGC-3'

The amplified product was subcloned into the pmCherry-N1 (Clontech Laboratories Inc.) vector by using BglII and EcoRI restrictions sites. Amino acid sequence of the human $P2X_4$ receptors fully corresponds to the isoform 3 described in gene database of the National Institute of Health.

Cell culture and establishment pmCherry-N1-h$P2X_4$ expressing HEK 293 cell clones

Human embryonic kidney (HEK) 293 cells were grown in plastic tissue culture flasks in DMEM/Ham's F-12 (1:1) medium supplemented with 5% fetal bovine serum, 100 U/ml penicillin and 100µg/ml streptomycin at 37°C in a cell culture incubator supplied with 5% CO_2. Cells were subcultivated when confluency reached 90-95%. To establish pmCherry-N1-hP2X4 expressing HEK 293 cell clones, cells plated the day before on poly-D-lysine coated 35 mm dish were transfected with 2 µg pmCherry-N1-h$P2X_4$ using 5 µl Lipofectamine 2000 per well as described in the manufacturer's protocol. Transfection medium was changed to antibiotic-free medium after 4 hours. On the following day the medium was then changed with selection antibiotic (G418) containing medium. From then on, the cells were kept in this selection medium. After a massive cell death of the non-transfected cells, surviving cells were trypsinized and replated in a 96-well plate at such a dilution that 1 cell/well density was obtained. After several days, colonies of cells displaying red fluorescence were selected as $hP2X_4$-expressing positive clones using fluorescence microscopy.

Transient transfection

Before the day of transfection, cells were plated on poly-D-lysine coated round glass coverslips (25 mm in diameter) at a density of 500,000 cells in 40 mm plastic Petri dishes. After 16-24 h, cells were transfected with 3µg pmCherry-N1-h$P2X_4$ DNA and 5µl of TurboFect™ transfection reagent in 200µl of serum-free medium. Cells were subjected to experiments 16-48 h after transfection. The efficiency of transfection was 60-70%.

Cell surface biotinylation and western blotting

$P2X_4$ expressing HEK 293 cell clones were plated at 1.000.000 cell density into poly-D-lysine coated 60 mm dishes. 24 hours after plating, cells were rinsed with ice-cold PBS-Ca-Mg (PBS containing 0.1 mM $CaCl_2$ and 1 mM $MgCl_2$) followed by biotinylation of proteins at the plasma membrane with 1.5 mg/ml sulfo-NHS-LC-biotin in 10 mM triethanolamine (pH 7.4), 1 mM $MgCl_2$, 2 mM $CaCl_2$, and 150 mM NaCl for 90 minutes with horizontal shaking at 4°C. Next, excess biotin was quenched with PBS containing 1 mM $MgCl_2$, 0.1 mM $CaCl_2$, and 100 mM glycine for 20 minutes at 4°C, and then rinsed three times with PBS. Cells were finally lysed in lysis buffer for 30 minutes and lysates were cleared by centrifugation. Protein concentrations were determined by DC Protein Assay. Portion of cell lysates of equivalent amounts of protein (1.33 mg/ml) were equilibrated overnight with streptavidin agarose beads at 4°C. Beads were washed sequentially with *solutions A* [50 mM Tris·HCl (pH 7.4), 100 mM NaCl, and 5 mM EDTA] three times, *B* [50 mM Tris·HCl (pH 7.4) and 500 mM NaCl] twice, and *C* (50 mM Tris·HCl, pH 7.4) once. Biotinylated surface proteins were then released by heating to 95°C with 4x Laemmli buffer. Proteins from the intracellular fraction were also heated to 95°C for 5 minutes with 4x Laemmli buffer.

Samples were run on a 10% SDS gel with 40 µl protein loaded from the cytosolic protein (1 mg/ml) and the plasma membrane samples. Samples were transferred onto a PVDF membrane in Towbin's buffer using the semi-dry transfer method. Membranes were blocked with PBS containing 5% milk, 0.5% BSA and 0.02% NaN_3 at room temperature for 1 hour. Afterwards, samples were incubated in blocking solution containing the appropriate primary antibody (1:1000 for mouse anti-mCherry (Clontech, 632543)) at 4°C for overnight followed by three washes with PBST. HRP-conjugated goat anti-mouse antibody (1:4000, BioRad) was used as secondary antibody. After three consecutive washes with PBST and a final wash

with PBS, the enhanced chemiluminescence (ECL) method was used for detection. For loading control the membrane probed with anti-mCherry was stripped and blotted with avidin-HRP (1:1000, BioRad).

Histochemistry

After 24 hours of plating 400.000 $P2X_4$-expressing HEK 293 clonal cells into a 35 mm dish, cells were washed thoroughly with PBS. Next, cells were incubated with 0.1 mg/ml LC-sulfo-NHS(+)-biotin (Molbio) at room temperature for 1 hour followed by three washes with PBS. Thereafter, cells were fixed with 4% PFA at 37^0C for 15 minutes. Cells were washed three times with PBS before staining with Streptavidin conjugated to Alexa 488 (1:4000 dilution, Invitrogen) at room temperature for one hour. After washing the cells four times with PBS, samples were mounted with CitiFluor AF2 (EMS). Images were captured with a Nikon C1 confocal laser scanning microscopy system equipped with Multiline Argon and HeNe lasers using 40x magnification.

Measurement of intracellular calcium levels

Transiently transfected HEK 293 cells were loaded with Fluo-3/AM (4µl) in standard extracellular solution for 45 min at room temperature. Fluorescence dye was dissolved in DMSO containing 20% Pluronic-F127. Additionally, the loading solution contained 1 mM probenecid to prevent dye leakage. After dye loading, cells were washed with standard extracellular solution. Standard extracellular solution contained (in mM): 145 NaCl, 5 KCl, 2 $CaCl_2$, 1 $MgCl_2$, 10 D-glucose and 10 HEPES, pH 7.4 (with NaOH). Nominally Ca^{2+}-free solutions were prepared by simply omitting $CaCl_2$.

Measurements were performed with a Axiovert 200 M Zeiss LSM 510 Meta (Carl Zeiss, Jena, Germany) confocal laser scanning microscope equipped with a 20x Plan Apochromat (NA=0.80) DIC objective. For the excitation, 488-nm argon-ion laser was used. The emitted light was collected with BP 505-570 band pass filter. Data were obtained at a rate of 0.5 Hz. Changes in $[Ca^{2+}]_i$ are displayed as the percentage of fluorescence relative to the intensity at the beginning of each experiment. The baseline fluorescence (100 %) was calculated from the average fluorescence of ROIs while bathing the cells with standard extracellular solution. Background fluorescence was subtracted from fluorescence intensity by measuring a cell-free area on every coverslip. Agonists and antagonists were administered directly to the solution at the desired concentrations. All experiments were done at room temperature (22-24 °C).

Fluorescence ion measurement experiments using FLIPRTetra

Cells were trypsinized and plated at 40,000 cells/well density in 100 µl volume onto 96-well black plates coated with 100µg/ml poly-D-lysine 36 hours before the experiments. HEK 293 cells were used for testing the effects of compounds on endogenous P2Y receptors; whereas $P2X_4$ activity was measured using $P2X_4$-expressing HEK 293 cell clones. 36 hours later the medium was replaced with 100 µl of loading buffer (modified Krebs buffer containing 117 mM NaCl, 4,8 mM KCl, 1 mM $CaCl_2$,1 mM $MgCl_2$, 5 mM D-glucose, 10 mM HEPES, and Calcium-5 fluorescence dye). Cells were then incubated in the loading buffer at 37°C for one hour. Fluorescence calcium measurements were carried out using FLIPTetra high-throughput, fluorescence microplate reader. Cells were excited using a 470-495 nm LED module, and the emitted fluorescence signal was filtered with a 515-575 nm emission filter. After establishment of a stable baseline, cells were incubated with the compounds for five minutes followed by the administration of ATP with or without the tested compounds.

Electrophysiology

Voltage-clamp recordings were carried out in the standard whole-cell configuration using an Axopatch 200B amplifier (Axon Instruments) [32]. Human $P2X_4$-expressing cells were selected using a Diaphot 300 inverted patch clamp microscope (Nikon) equipped with an epifluorescent attachment (Elektro-Optika, Érd, Hungary). Micropipettes were pulled by a P-97 Flaming-Brown type micropipette puller (Sutter Instrument) from borosilicate glass capillary tubes (Harvard Apparatus) and had a tip resistance of 3–6 MΩ when filled with pipette solution. Patch pipette filling solution contained (in mM): 135 KCl, 5 NaCl, 1 $MgCl_2$, 1 EGTA, 10 HEPES and an appropriate concentration of $CaCl_2$, to give free $[Ca^{2+}]_i$ = 0.1 µM. Free $[Ca^{2+}]_i$ was estimated using MaxChelator software (Stanford University, Palo Alto, USA). The pH was adjusted to 7.2 with KOH. Standard extracellular solution contained (in mM): 145 NaCl, 5 KCl, 2 $CaCl_2$, 1 $MgCl_2$, 10 D-glucose, 10 HEPES, pH 7.4 (with NaOH). Solutions were delivered by continuous perfusion with a gravity-fed delivery system. Antagonists were added to the bath solutions 3-5 min. prior to agonist application.

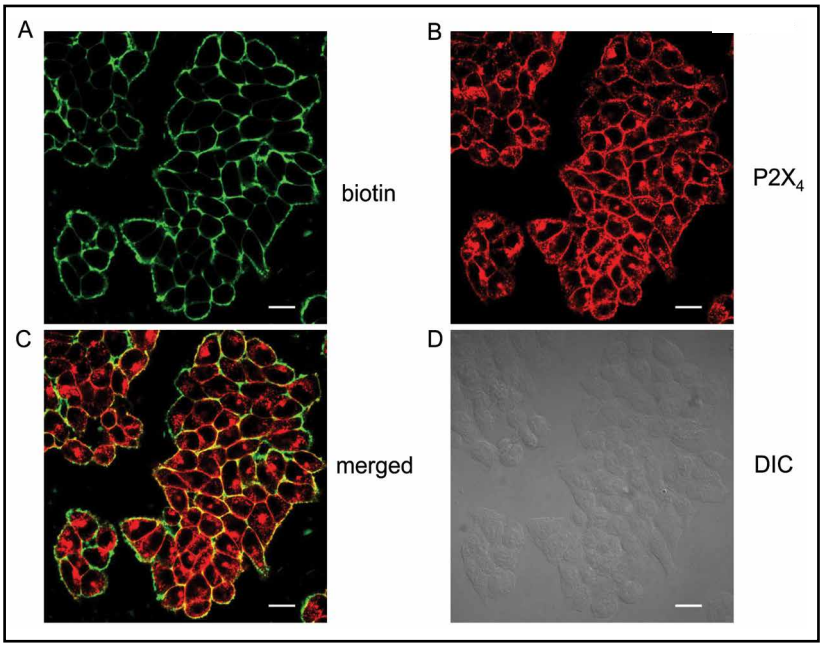

Fig. 1. Cellular localization of $P2X_4$Rs by immunohistochemistry. Panel A: Cell surface proteins stained with LC-sulfo-NHS(+)-biotin and streptavidin-Alexa488. Panel B: Fluorescence image of mCherry tagged $P2X_4$Rs in HEK 293 cells. Panel C: Merged image showing co-localization of $P2X_4$Rs and biotinylated cell surface proteins. Panel D: Differential interference contrast (DIC) image of the $P2X_4$Rs expressing cells. Scale bar represents 20 μm.

Experiments were performed at a holding potential of -60 mV. Command protocols and data acquisition were controlled by pClamp 6.03 software (Axon Instruments). Capacitative currents were compensated with analog compensation. Series resistance was accepted if lower than five times the pipette tip resistance. Analog data were filtered at 1 kHz with a low-pass Bessel filter and digitized at 5 kHz using a Digidata 1200 interface board. Data were analyzed using Clampfit 6.03 and Microsoft Excel softwares. All experiments were performed at room temperature.

Data presentation

Areas under the curve (AUC) values were calculated using the trapezoidal rule, in the first 4 minutes following agonist application (SigmaPlot 12.0 software). To estimate P2X receptor function, non-expressing cell responses were subtracted from the AUC values obtained in $P2X_4$R expressing cells on the same coverslip.

Antagonist concentration-inhibition curves were obtained by using progressively increasing antagonist concentrations and a fixed agonist concentration close to the EC_{50} unless otherwise stated. IC_{50} values were calculated by least squares fitting to $I = I_0/[1 + (IC_{50}/[Ant])^{-nH}]$, where I and I_0 represent peak responses in the presence and absence of antagonist at concentration [Ant].

Results were presented as means ± SEM of n observations if not otherwise indicated. Statistical significance was determined using paired Student's t-test for parametric, whereas one-way ANOVA followed by Mann-Whitney U test for non-parametric variables. Differences were considered statistically significant when $p < 0.05$. Non-linear curve fitting was performed using the SigmaPlot 12.0 program.

Results

Localization and functional characterization of transfected $hP2X_4$ receptors in HEK 293 cells

In order to study the localization of transfected $hP2X_4$ receptors in HEK 293 cells we used immunohistochemical techniques. Co-localization of biotinylated cell surface proteins and mCherry fluorescent protein suggested the expression of $P2X_4$Rs in the plasma membrane (Fig. 1). Furthermore, cell surface biotinylation and western blotting were used to separate the cytosolic and membrane fractions of proteins in HEK 293 cells. The $P2X_4$-bound mCherry protein was detected at the plasma membrane and its expression was not altered by the presence of ivermectin (Fig. 2A). In control experiment we used avidin-HRP-conjugated antibody to confirm the localization of proteins in the membrane fraction (Fig. 2B).

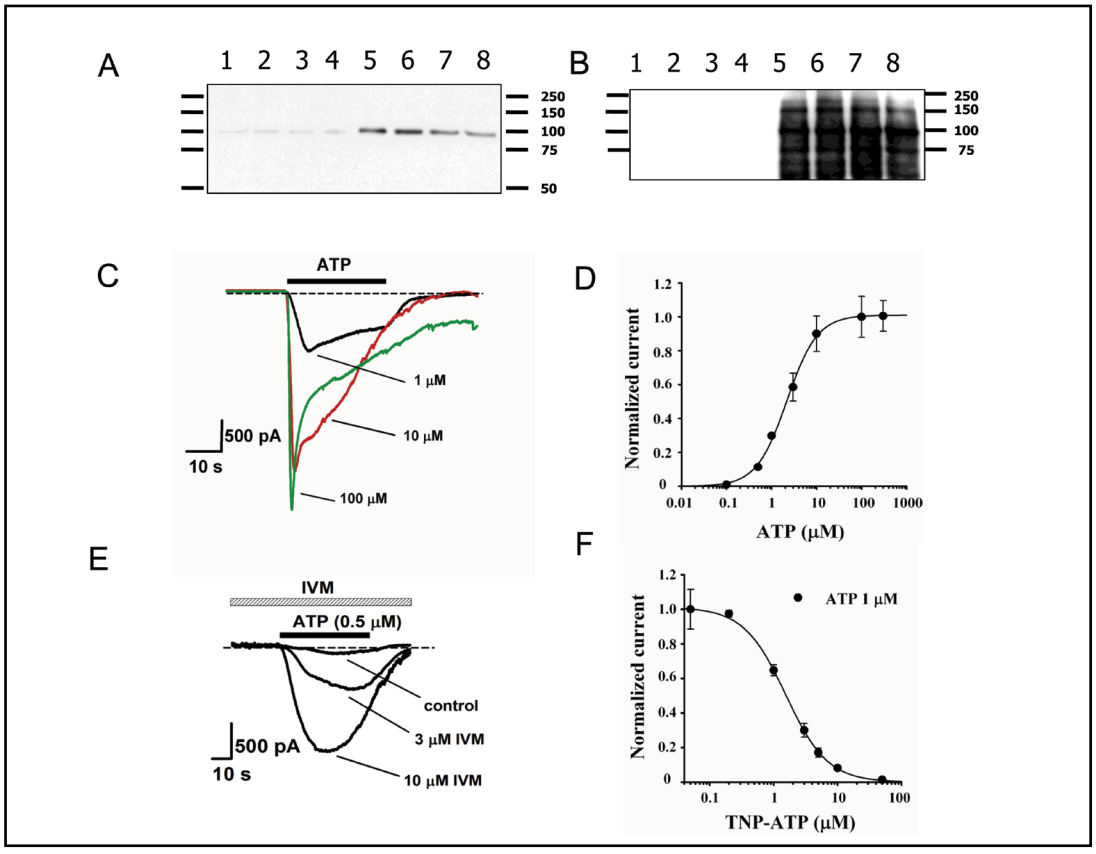

Fig. 2. Localization and functional characterization of transfected hP2X$_4$ receptors in HEK 293 cells. Panel A: Cytosolic and cell surface proteins were separated. Human P2X$_4$Rs are expressed both in cytosolic (lanes 1-4) and plasma membrane (lanes 5-8) fractions of proteins. Lane 1 and 5 indicate unstimulated cells, lanes 2 and 6 DMSO-pretreated (1:1000) cells, lanes 3 and 7 IVM-pretreated (10 μM) cells and lanes 4 and 8 IVM-pretreated (20 μM) cells. Panel B: In control experiments we obtained protein expression only in cell surface fraction (lanes 5-8) using avidin-HRP. Panel C: Representative traces showing ATP-induced inward currents in the absence; and panel E: presence of ivermectin (IVM). Panel D: Concentration-responses to ATP (0.1-300 μM) are shown. Panel F: Concentration-inhibitions to TNP-ATP (0.05-50 μM) in ATP-stimulated (1 μM) cells are shown. Values are means ± SEM. The error bars are not always visible due to the small SEM values. Experiments at each concentration were performed at least 3 times.

To functionally characterize the plasma membrane localized hP2X$_4$ receptors we measured whole cell currents in transfected HEK 293 cells. ATP (0.1-300 μM) elicited increasing maximal current amplitudes in cells expressing P2X$_4$Rs (Fig. 2C and D). The agonist concentration-response curve for ATP were fit with the Hill-equation; $E = E_{max}[1 + (EC_{50}/[A])^{nH}]$ where E stands for the peak current evoked by agonist concentration $[A]$, E_{max} is the peak current evoked by a maximal agonist concentration, EC_{50} is the concentration giving half the maximal current, and nH represents the Hill coefficient. Our results showed that the EC_{50} value of ATP was 2.1 μM (Fig. 2D). Cells lacking P2X$_4$R expression failed to respond to ATP (100 μM) (data not shown). To confirm the role of P2X$_4$Rs in ATP-induced inward currents we pretreated the cells with ivermectin (IVM) (3 and 10 μM). As expected, IVM potentiated currents induced by ATP (0.5 μM) in a concentration-dependent manner (Fig. 2E). In addition, we tested the effects of TNP-ATP on ATP-induced (1 μM) currents. Under these conditions, we found that the half-maximal inhibitory concentration (IC_{50}) of TNP-ATP was 1.5 μM (Fig. 2F). These data show the plasma membrane localized hP2X$_4$ receptors are fully functional in transfected HEK 293 cells.

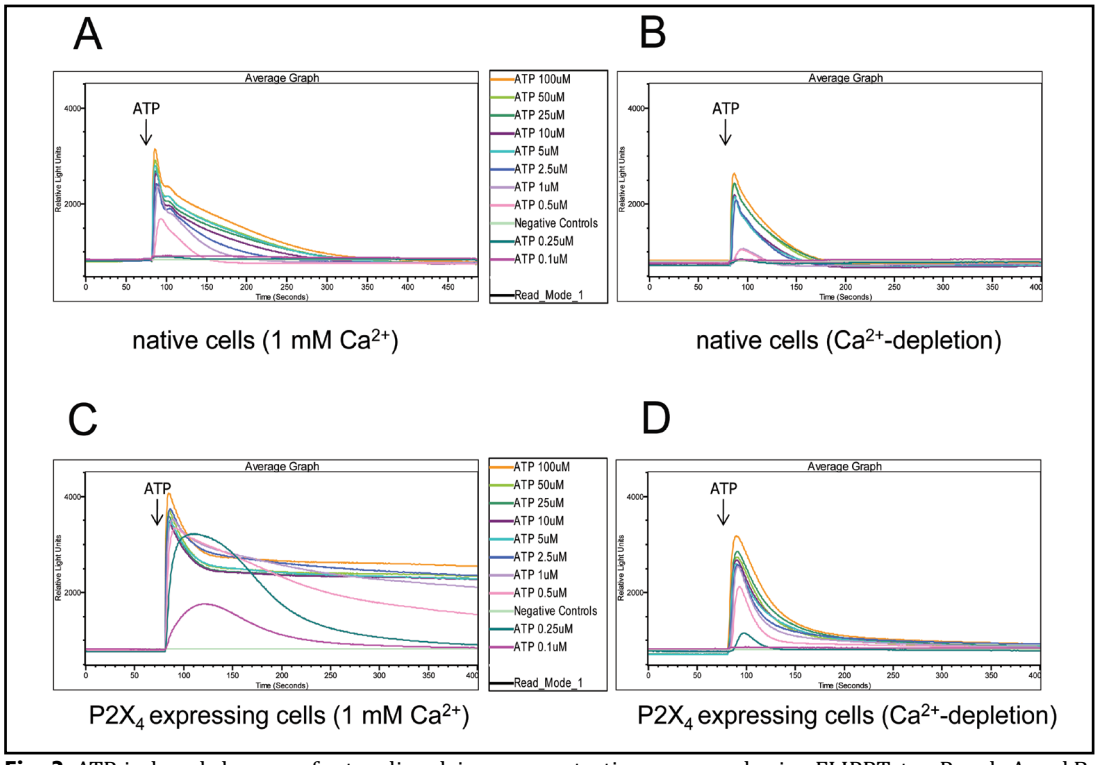

Fig. 3. ATP-induced changes of cytosolic calcium concentration measured using FLIPRTetra. Panels A and B: Administration of extracellular ATP induced dose-dependent, similar transient changes of cytosolic calcium in HEK 293 cells in the presence or absence of extracellular calcium. Panel C: In contrast, in HEK 293 cells stably expressing hP2X$_4$ ATP-induced sustained calcium response in the presence of extracellular calcium Panel D: whereas in calcium-free buffer the responses were similar to the ones obtained in non-transfected cells. Average tracings of 6 individual experiments are shown.

ATP-induced Ca^{2+} influx is inhibited by 5-BDBD in cells stably expressing P2X$_4$Rs

In native HEK 293 cells ATP (0.5-100 μM) caused transient increases in cytosolic calcium concentrations whereas lower doses of the agonist (0.1-0.25 μM) elicited no change in calcium levels (Fig 3A). In nominally calcium-free buffer ATP (0.1-100 μM) caused similar effects suggesting that the calcium signal was due to P2Y receptor-dependent Ca^{2+} release from the intracellular stores (Fig. 3B). Although the presence of external Ca^{2+} prolonged ATP-induced calcium signals, sustained responses could not been observed (Fig. 3A). Next, we studied ATP-induced Ca^{2+} signals in HEK 293 cell clones stably expressing P2X$_4$Rs (see methods). In these cells ATP (0.1-0.25 μM) elicited changes in Ca^{2+} concentrations that were abolished in Ca^{2+}-depleted medium indicating that Ca^{2+} entered the cells from the extracellular space (Fig. 3C and D). In addition, higher concentrations of ATP (≥ 1μM) caused sustained Ca^{2+} signals (Fig. 3C). Importantly, the P2X$_4$ receptor-specific positive allosteric modulator IVM (20 μM) potentiated the ATP-induced (0.25 μM) Ca^{2+} entry (AUC_{ATP} = 852 ± 47; n=5 vs. $AUC_{ATP+IVM}$ = 1026 ± 46; n=5; $p<0.05$). These data indicate that using low concentrations of ATP (≤0.25 μM) allows assessment of P2X$_4$R-mediated Ca^{2+} signals independent of P2Y receptor activation. Thus, we next studied the effects of the benzodiazepine derivative 5-BDBD in the presence of 0.25 μM ATP. Under these conditions 5-BDBD (2-20 μM) significantly inhibited P2X$_4$R-mediated Ca^{2+} entry (Fig. 4A). We obtained similar inhibitory effects of 5-BDBD when cells were stimulated by 0.5 μM ATP (Fig. 4B). Regardless of ATP concentrations used, 5-BDBD (1-20 μM) had no effects in native HEK 293 cells suggesting that endogenously expressed P2Y receptors were not inhibited (data not shown).

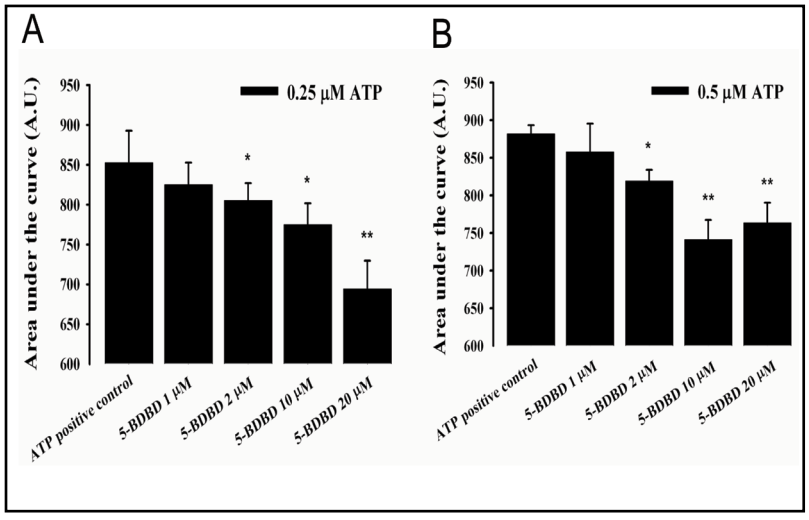

Fig. 4. 5-BDBD inhibited the ATP-induced Ca^{2+} signals in HEK 293 cells stably expressing $hP2X_4$ receptors. Panels A and B: Concentration-dependent inhibition of Ca^{2+} signals by 5-BDBD when cells were stimulated with 0.25 μM and 0.5 μM ATP. Values are means ± SD. Each experiment was performed at least 4 times. A.U. means arbitrary units. *p<0.05 and **p<0.005 vs. ATP positive controls (ANOVA).

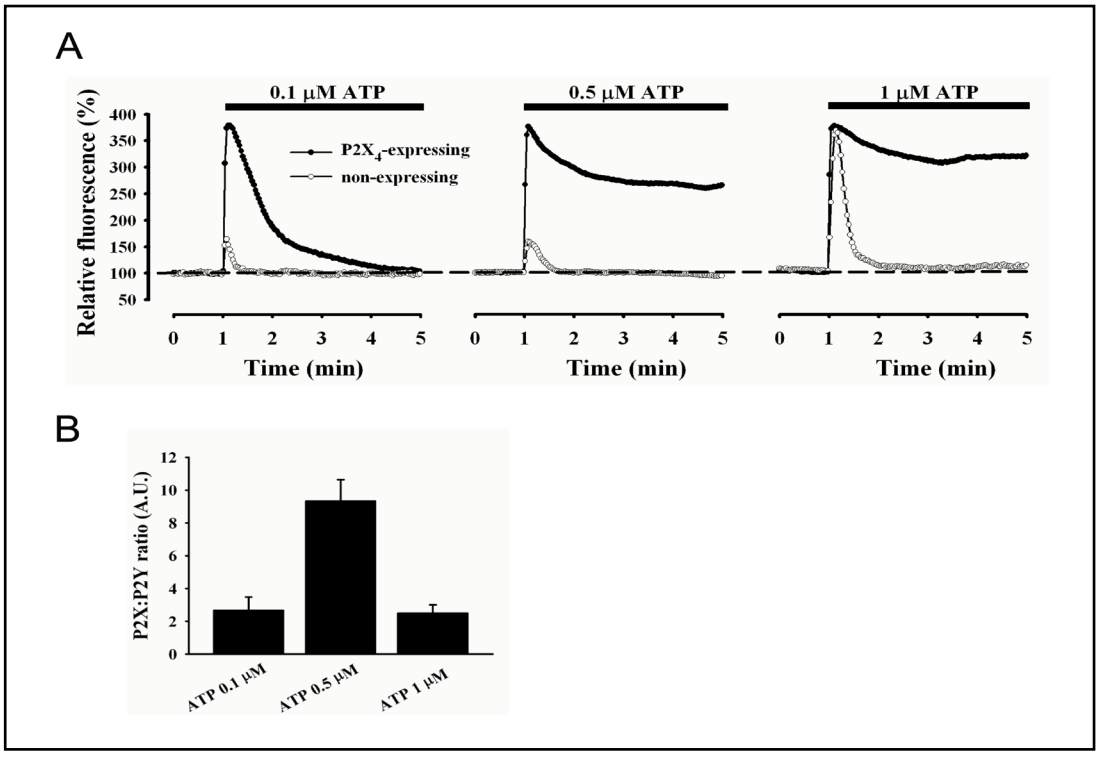

Fig. 5. ATP induced concentration-dependent changes in $[Ca^{2+}]_i$ in $hP2X_4$-expressing and non-expressing HEK 293 cells. Panel A: Representative traces showing the effects of different ATP concentrations (0.1-1μM) on $[Ca^{2+}]_i$ Each experiment was performed at least 5 times; Panel B: P2XR:P2YR-mediated Ca^{2+} response ratios are shown at different ATP concentrations. P2YR-mediated responses were estimated by the amplitude of cytosolic Ca^{2+} peaks while P2XR-mediated responses were assessed by "area under the curve" (AUC) values referring to the sustained nature of the Ca^{2+} signal. S.E.M. values are not shown for the representative traces because they were within 10% of the mean. A.U. means arbitrary units.

Single cell calcium imaging in cells transiently expressing $P2X_4$Rs

Single cell calcium imaging has been shown to provide an alternative method for the assessment of P2X receptor channel activity [33]. Therefore, we also studied the ATP-induced intracellular Ca^{2+} signals at the single cell level. In order to conduct simultaneous measurements of cytosolic Ca^{2+} levels in $P2X_4$R-expressing and non-expressing cells, we used

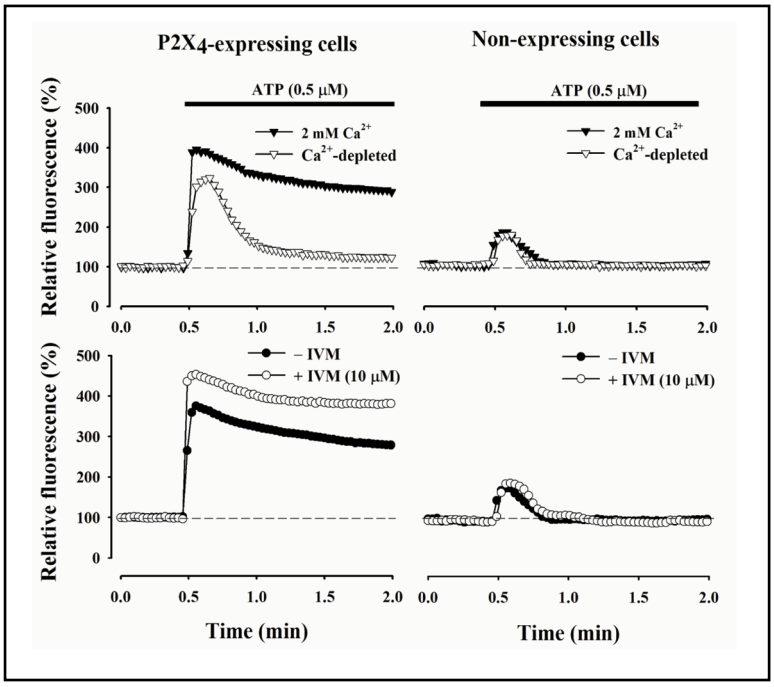

Fig. 6. Top panels: ATP induced changes in $[Ca^{2+}]_i$ in Ca^{2+}-containing or Ca^{2+}-depleted medium. Bottom panels: Ivermectin (IVM) potentiated the ATP-induced Ca^{2+} signal only in $hP2X_4$-expressing cells.

the transient transfection method. First, we identified the extracellular ATP concentration at which P2XR:P2YR-mediated Ca^{2+} response ratio was the highest. The P2YR-mediated responses were estimated by the amplitude of cytosolic Ca^{2+} peaks while P2XR-mediated responses were assessed by "area under the curve" (AUC) values referring to the sustained nature of the Ca^{2+} signal. In cells lacking $P2X_4R$ expression, administration of 0.1 μM and 0.5 μM ATP evoked small peak increases without sustained Ca^{2+} signals (Fig. 5A). In cells expressing $P2X_4Rs$, the magnitude of Ca^{2+} peaks induced by 0.1 μM and 0.5 μM ATP were significantly higher than in non-expressing cells. However, robust Ca^{2+} plateau was induced only by 0.5 μM ATP (Fig. 5A). Further increasing ATP concentrations (1 μM), a considerable rise in cytosolic Ca^{2+} peak was observed in cells lacking $P2X_4R$ expression. In contrast, the sustained component of the Ca^{2+} signal induced by 1 μM ATP did not significantly differ from that elicited by 0.5 μM ATP in $P2X_4R$ expressing cells (Fig. 5A). Consequently, as P2XR:P2YR-mediated Ca^{2+} response ratio was the highest at 0.5 μM ATP (Fig. 5B), in subsequent experiments this concentration was chosen to investigate single cell Ca^{2+} signals. To demonstrate that extracellular Ca^{2+} was necessary for ATP-induced sustained Ca^{2+} signal in cells expressing $P2X_4Rs$, we repeated the experiments in Ca^{2+}-depleted medium. Under these circumstances, the Ca^{2+} signal was only transient suggesting that Ca^{2+} entry was due to functional expression of $P2X_4Rs$ (Fig. 6). In cells lacking $P2X_4R$ expression, external Ca^{2+} did not influence the ATP-induced transient nature of cytosolic Ca^{2+} signal (Fig. 6). These data excluded the possibility that store-operated calcium channels played significant role in Ca^{2+} entry when cells were stimulated with 0.5 μM ATP. To further characterize the sustained Ca^{2+} signal, we pretreated the cells with IVM (10 μM) 5 min prior the application of ATP. Our results showed that ATP-induced Ca^{2+} plateau was significantly elevated in $P2X_4R$ expressing but not in non-expressing cells (Fig. 6).

Next, we tested the effects of 5-BDBD on ATP-induced (0.5 μM), $P2X_4R$-mediated Ca^{2+} entry. Sustained Ca^{2+} signals were diminished in cells pretreated with different concentrations of 5-BDBD (0.5-20 μM). We observed 50% reduction of the AUC values in the presence of approx. 2 μM 5-BDBD (Fig. 7A). We also studied inhibitory effects of TNP-ATP which was reported as a putative antagonist of $P2X_4Rs$ [25]. As shown in Figure 7B, TNP-ATP (0.5-50 μM) reduced ATP-induced (0.5 μM) sustained Ca^{2+} signal in a concentration-dependent manner. Taken together, these data indicate that ATP-induced sustained Ca^{2+} signals were inhibited by both 5-BDBD and TNP-ATP in HEK 293 cells transfected with $P2X_4Rs$.

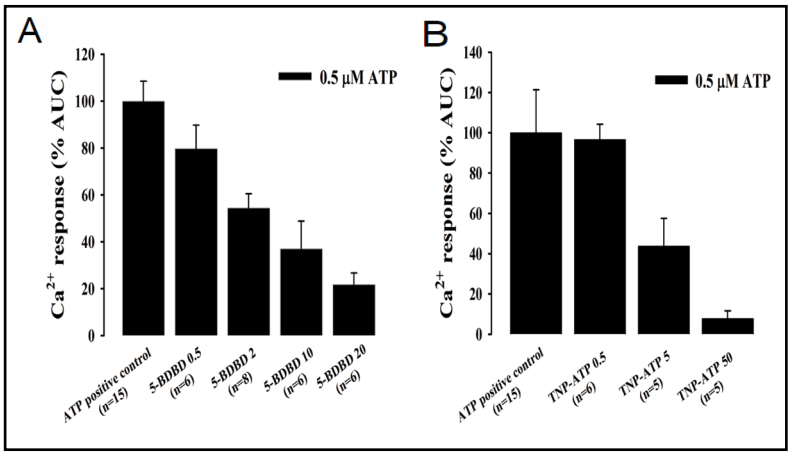

Fig. 7. Both 5-BDBD and TNP-ATP inhibited the ATP-induced Ca^{2+} signals in HEK 293 cells transiently transfected with $hP2X_4$ receptors. Panels A and B: Concentration-dependent inhibition of the ATP-induced Ca^{2+} response by 5-BDBD (0.5-20μM); and TNP-ATP (0.5-50μM). The number of independent experiments is indicated in parenthesis beneath the columns.

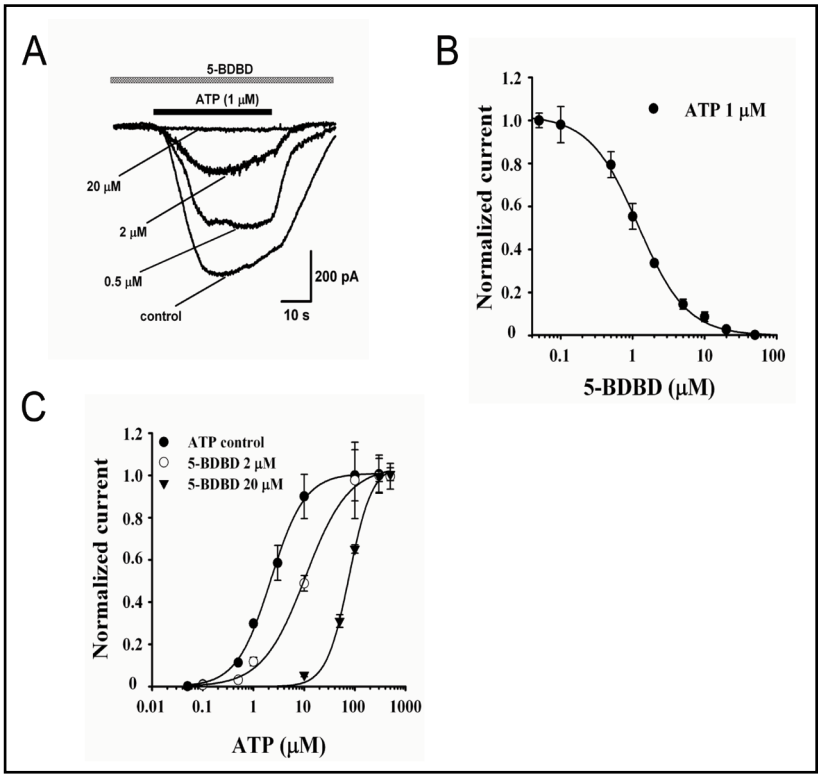

Fig. 8. 5-BDBD competitively inhibited the ATP-induced whole cell inward ion currents in HEK 293 cells transiently expressing $hP2X_4$ receptors. Panel A: Representative original traces showing the inhibitory effects of 5-BDBD at various concentrations. Panel B: Concentration-dependent inhibition of 5-BDBD (0.1-50 μM) in ATP-stimulated (1 μM) cells are shown. Panel C: Concentration-dependent responses to ATP (0.1-300 μM) in cells that were pretreated with 2 or 20 μM 5-BDBD. The rightward shift of the ATP control curve and the unchanged maximal stimulation suggest that 5-BDBD competitively inhibited the $P2X_4$ receptor channels. In the absence of 5-BDBD the Hill coefficient was 1.26. In the presence of 2 μM and 20 μM 5-BDBD nH values were 1.11 and 2.17, respectively. Values are means ± SEM. The error bars are not always visible due to the small SEM values. Experiments at each concentration were performed at least 3 times.

$P2X_4$ receptor channels are competitively inhibited by 5-BDBD

Data presented in this paper show that 5-BDBD inhibited the $P2X_4$R-mediated Ca^{2+} entry in both stably and transiently transfected HEK 293 cells (see above). Nonetheless, during measurements of intracellular Ca^{2+} concentrations activation of endogenous P2YRs and/or ion transporters that eliminate Ca^{2+} from the cytosol (i.e. plasma membrane Ca^{2+}-ATPase, sarcoplasmic reticulum Ca^{2+}-ATPase) might possibly interfere with the effectiveness of 5-BDBD. Therefore, we also tested the inhibitory effects of 5-BDBD in HEK 293 cells using the whole cell configuration of the patch clamp technique. We stimulated the cells with 1 μM

ATP (close to EC_{30} of ATP) because higher concentrations of the agonist induced premature cell damage in a number of experiments. Under these circumstances, 5-BDBD (0.1-50 μM) dose-dependently inhibited $P2X_4R$-mediated inward currents ($I_{control}$: 1239 ± 105 pA, n=8 vs. $I_{0.5\mu M}$: 983 ± 148 pA, n=4 vs. $I_{2\mu M}$: 417 ± 33, n=4 vs. $I_{20\mu M}$: 13 ± 1 pA, n=4) with an IC_{50} of 1.2 μM (Fig. 8A and B). To investigate whether the inhibitory effect of 5-BDBD was due to competitive or allosteric interaction with $P2X_4Rs$, we performed additional electrophysiological experiments. Application of two different concentrations of 5-BDBD (2 μM and 20 μM) caused a rightward shift in ATP dose-response curve (from EC_{50} = 2.1 μM to 11.2 μM and 79.2 μM, respectively, using non-linear regression analysis). Since the magnitude of maximal stimulation did not change, these data suggest that 5-BDBD competitively inhibited the $P2X_4Rs$ (Fig. 8C).

Discussion

$P2X_4$ receptors are involved in important physiological and pathophysiological functions such as afferent signalling, chronic pain and autocrine/paracrine communications of endothelial and epithelial cells. In these processes, investigations on the role of $P2X_4Rs$ are often hindered by lack of selective inhibitors. In recent years, considerable efforts have been made to discover novel effective antagonists of $P2X_4Rs$. Although the benzodiazepine derivative 5-BDBD has been recently proposed to selectively block $P2X_4Rs$ [27], only limited experiences have been available concerning its inhibitory properties [28-31]. Moreover, to the best of our knowledge, there are no previous studies attempting to compare the inhibitory effects of 5-BDBD using both electrophysiological and intracellular calcium measurements. Therefore, we aimed to investigate the inhibitory potency of 5-BDBD on $P2X_4R$-dependent Ca^{2+} entry. Our data provide evidence for competitive though moderate inhibitory effects of 5-BDBD. Depending on experimental conditions the degree of inhibition varied significantly. In patch clamp experiments, assessing the effects of 5-BDBD directly on its target protein, we obtained the strongest inhibition. In intracellular calcium measurements, 5-BDBD exhibited more robust effects in transiently transfected cells. This was probably due to both the higher level of $P2X_4R$ expression and the single cell calcium measurements. However, it is important to emphasis that AUC values are not in a linear fashion with $[Ca^{2+}]_i$ and quantitative analyses of fluorometric Ca^{2+} assay may provide only a rough orientation.

Despite the endogenous expression of at least three different P2Y receptor subtypes [34, 35] HEK 293 cells are frequently used to study properties of P2X receptors [34, 36]. To assess the role of P2XRs in inducing changes of intracellular Ca^{2+} concentrations, some investigators often choose cell lines (i.e. excitable mouse immortalized gonadotropin-releasing hormone-secreting cells (GT1) and human astrocytoma cells (1321N1)) that are lacking P2Y receptors [33, 37]. Stojilkovic and his colleagues transfected both GT1 and HEK 293 cells with different P2X subtypes and compared ATP-induced Ca^{2+} signals. They concluded that intracellular Ca^{2+} measurements could be used for the characterization of P2X receptors only in GT1 but not in HEK 293 cells because activation of endogenously expressed P2Y receptors interferes with P2X receptor-mediated Ca^{2+} signals [33]. This is indeed the case when HEK 293 cells are stimulated with high concentrations of ATP (>10 μM). Nonetheless, here we propose an alternative approach to investigate P2XR functions in HEK 293 cells applying low doses of agonist. In the present study, we show that submicromolar concentrations of ATP (≤ 0.25 μM) cause changes in intracellular Ca^{2+} concentrations solely in $P2X_4R$ expressing cells. The ATP-induced increase in Ca^{2+} concentrations was further enhanced by pretreatment of ivermectin and was completely abolished in Ca^{2+}-depleted medium suggesting that $P2X_4Rs$ were involved in Ca^{2+} influx. Furthermore, we found that higher doses of ATP (≥1 μM) prolonged the duration of Ca^{2+} signals in native HEK 293 cells. These effects were abolished in Ca^{2+}-depleted medium suggesting the activation of $P2X_4R$-independent Ca^{2+} influx mechanisms. The significantly higher initial phase of Ca^{2+} response in $P2X_4R$ expressing cells compared to native cells was probably due to the fact that we used

nominally Ca^{2+} free solutions. Nonetheless, according to our previous experience, we could not add calcium chelators because HEK 293 cells require extracellular Ca^{2+} to remain attached to the coverslip. We assume that, as a result of P2Y receptor-dependent Ca^{2+} release, store-operated Ca^{2+} entry could contribute to the overall Ca^{2+} signal when cells are stimulated with higher concentrations of ATP (>1 μM). Therefore, our results suggest that when sufficiently low ATP concentrations are applied, measurement of intracellular Ca^{2+} concentrations is a useful approach to assess properties of P2XR in HEK 293 cells.

Considering the fact that Ca^{2+} measurement in stably transfected cells did not allow concurrent investigations of the $P2X_4R$-expressing and non-expressing cells, we also performed single cell calcium measurements in transiently transfected HEK 293 cells. Thus, we could simultaneously measure ATP-induced Ca^{2+} signals in $P2X_4R$-expressing and non-expressing cells on the same coverslip. Our data suggest that up to the concentration of 0.5 μM, ATP causes only small transient changes in Ca^{2+} concentration whereas 1 μM ATP significantly enhances the signal amplitude in non-expressing cells. This phenomenon was probably due to the gradual activation of different endogenous P2Y receptor subtypes [35].

To our surprise, we found that amplitudes of ATP-induced Ca^{2+} signals were significantly higher in $P2X_4R$-expressing than in non-expressing cells when experiments were performed in Ca^{2+}-depleted medium (Fig. 6). Since we obtained similar results in stably transfected cells as well, we speculate that the difference was due to $P2X_4R$-mediated Ca^{2+} entry rather than additional release of Ca^{2+} from the internal stores. High levels of $P2X_4R$-expression and lack of Ca^{2+}-chelation could both contribute to the Ca^{2+} entry. Furthermore, our data show that IVM enhances the ATP-induced Ca^{2+} entry only in $P2X_4R$-expressing cells. In accordance with previous observations, IVM potentiated ATP-induced Ca^{2+} entry but did not increase surface expression of P2X4Rs [38, 39].

Our electrophysiological data confirmed the presence of functional $P2X_4Rs$ in transiently transfected HEK 293 cells. ATP caused IVM-sensitive activation of inward currents in $P2X_4R$-expressing but not in non-expressing cells. We found EC_{50} value of ATP close to what was previously reported [26]. However, it is noteworthy that, in some experiments ATP-stimulated currents exhibited incomplete recovery following withdrawal of the agonist when its concentration was higher than 1 μM. This was probably due to the high level of $P2X_4R$ expression and massive Ca^{2+} influx which could consequently cause cellular damage. Therefore, inhibitory properties of both TNP-ATP and 5-BDBD were tested at 1 μM ATP stimulation.

Activation of $P2X_4Rs$ plays a key role in the pathogenesis of neuropathic pain [15]. In an attempt to mitigate the neuropathic pain Inoue and his colleagues investigated the possible role of antidepressants as inhibitors of $P2X_4Rs$ [37]. They found that paroxetine inhibited $P2X_4Rs$ dose-dependently. Paroxetine behaved as a noncompetitive antagonist with IC_{50} values of 2.5 μM and 1.9 μM for rat and human $P2X_4Rs$, respectively. Interestingly, inhibitory effects of paroxetine were significantly stronger on rat $P2X_4Rs$ than that of TNP-ATP [37]. It is known that TNP-ATP is more than 1,000-fold more potent in blocking $P2X_1$ and $P2X_3$ than $P2X_4$ receptors [24]. Nonetheless, TNP-ATP has been used as $P2X_4$ antagonist in a number of studies [40, 41]. Our data also demonstrate that TNP-ATP inhibits both intracellular Ca^{2+} signals and inward ion currents induced by ATP. We found that TNP-ATP had an IC_{50} value of 1.5 μM for 1 μM ATP stimulation which was comparable with previous observations [25]. Noncompetitive antagonism of TNP-ATP at the $P2X_3Rs$ suggests similar mechanisms of action at $P2X_4Rs$ as well [25].

Recently, 5-BDBD has been proposed to selectively inhibit $P2X_4Rs$ [27]. Since then 5-BDBD has been used in a number of studies with contradictory results [28-31]. It has weak potency to inhibit recombinant human $P2X_4Rs$ [28] or native $P2X_4Rs$ in vascular endothelial cells (IC_{50} ~ 30 μM) [30]. In contrast, $P2X_4Rs$ were potently blocked by 10 μM 5-BDBD in prechondrogenic cell line [29]. Here we report that 5-BDBD and TNP-ATP have similar inhibitory potencies at recombinant human $P2X_4Rs$ expressed in HEK 293 cells. Our data suggest that 5-BDBD may competitively inhibit the $P2X_4Rs$. However, we cannot exclude the possibility that 5-BDBD decreases the ligand-binding affinity of the channels. Such allosteric

alterations of ATP-binding affinity have been previously reported for P2X receptors [42, 43].

In conclusion, the present study demonstrates that intracellular measurement of Ca^{2+} concentration in HEK 293 cells could be a useful method to investigate pharmacological properties of P2X receptor antagonists provided that submicromolar concentrations of ATP are used. 5-BDBD and TNP-ATP have similar inhibitory potencies at human recombinant $P2X_4$Rs. Our data show that 5-BDBD shifts the ATP concentration-response curve to the right. This feature differs from the previously described noncompetitive behavior of other $P2X_4$R antagonists such as TNP-ATP and paroxetine.

Acknowledgements

This work was supported by the OTKA K79189 grant and Swiss National Science Foundation (SNSF) through the National Centre of Competence in Research (NCCR) TransCure (website: http://www.transcure.org). The authors thank Péter Várnai and Dániel Tóth for their help to create the pmCherry-N1-h$P2X_4$ construct.

References

1 Schwiebert EM, Zsembery A: Extracellular ATP as a signaling molecule for epithelial cells, Biochim Biophys Acta 2003;1615:7-32.
2 Burnstock G, Fredholm BB, North RA, Verkhratsky A: The birth and postnatal development of purinergic signalling. Acta Physiol 2010;199:93-147.
3 Jo YH, Role LW: Coordinate release of ATP and GABA at in vitro synapses of lateral hypothalamic neurons. J Neurosci 2002;22:4794-4804.
4 Sim JA, Chaumont S, Jo J, Ulmann L, Young MT, Cho K, Buell G, North RA, Rassendren F: Altered hippocampal synaptic potentiation in P2X4 knock-out mice. J Neurosci 2006;26:9006-9009.
5 Khakh BS, Kennedy C: Adenosine and ATP: Progress in their receptors' structures and functions. Trends Pharmacol Sci 1998;19:39-41.
6 Roper SD: Signal transduction and information processing in mammalian taste buds. Pflugers Arch 2007;454:759-776.
7 Housley GD, Marcotti W, Navaratnam D, Yamoah EN: Hair cells--beyond the transducer. J Membr Biol 2006;209:89-118.
8 Rong W, Gourine AV, Cockayne DA, Xiang Z, Ford AP, Spyer KM, Burnstock G: Pivotal role of nucleotide P2X2 receptor subunit of the ATP-gated ion channel mediating ventilatory responses to hypoxia. J Neurosci 2003;23:11315-11321.
9 Di Virgilio F: Purinergic signalling in the immune system. A brief update. Purinergic Signal 2007;3:1-3.
10 Surprenant A, North RA: Signaling at purinergic P2X receptors. Annu Rev Physiol 2009;71:333-359.
11 Barclay J, Patel S, Dorn G, Wotherspoon G, Moffatt S, Eunson L, Abdel'al S, Natt F, Hall J, Winter J, Bevan S, Wishart W, Fox A, Ganju P: Functional downregulation of P2X3 receptor subunit in rat sensory neurons reveals a significant role in chronic neuropathic and inflammatory pain. J Neurosci 2002;22:8139-8147.
12 Cockayne DA, Dunn PM, Zhong Y, Rong W, Hamilton SG, Knight GE, Ruan HZ, Ma B, Yip P, Nunn P, McMahon SB, Burnstock G, Ford AP: P2X2 knockout mice and P2X2/P2X3 double knockout mice reveal a role for the P2X2 receptor subunit in mediating multiple sensory effects of ATP. J Physiol 2005;567:621-639.
13 Coull JA, Beggs S, Boudreau D, Boivin D, Tsuda M, Inoue K, Gravel C, Salter MW, De Koninck Y: BDNF from microglia causes the shift in neuronal anion gradient underlying neuropathic pain. Nature 2005;438:1017-1021.
14 Chizh BA, Illes P: P2X receptors and nociception. Pharmacol Rev 2001;53:553-568.
15 Tsuda M, Shigemoto-Mogami Y, Koizumi S, Mizokoshi A, Kohsaka S, Salter MW, Inoue K: P2X4 receptors induced in spinal microglia gate tactile allodynia after nerve injury. Nature 2003;424:778-783.
16 Labasi JM, Petrushova N, Donovan C, McCurdy S, Lira P, Payette MM, Brissette W, Wicks JR, Audoly L, Gabel CA: Absence of the P2X7 receptor alters leukocyte function and attenuates an inflammatory response. J Immunol 2002;168:6436-6445.
17 Mulryan K, Gitterman DP, Lewis CJ, Vial C, Leckie BJ, Cobb AL, Brown JE, Conley EC, Buell G, Pritchard CA, Evans RJ: Reduced vas deferens contraction and male infertility in mice lacking P2X1 receptors. Nature 2000;403:86-89.

18 Yamamoto K, Korenaga R, Kamiya A, Qi Z, Sokabe M, Ando J: P2X(4) receptors mediate ATP-induced calcium influx in human vascular endothelial cells. Am J Physiol Heart Circ Physiol 2000;279:H285-292.
19 Yamamoto M, Jin JJ, Wu Z, Abe M, Tabara Y, Nagai T, Yamasaki E, Igase M, Kohara K, Miki T, Nakura J: Interaction between serotonin 2A receptor and endothelin-1 variants in association with hypertension in japanese. Hypertens Res 2006;29:227-232.
20 Ma W, Korngreen A, Weil S, Cohen EB, Priel A, Kuzin L, Silberberg SD: Pore properties and pharmacological features of the P2X receptor channel in airway ciliated cells. J Physiol 2006;571:503-517.
21 Zsembery A, Fortenberry JA, Liang L, Bebok Z, Tucker TA, Boyce AT, Braunstein GM, Welty E, Bell PD, Sorscher EJ, Clancy JP, Schwiebert EM: Extracellular zinc and ATP restore chloride secretion across cystic fibrosis airway epithelia by triggering calcium entry. J Biol Chem 2004;279:10720-10729.
22 Liang L, Zsembery A, Schwiebert EM: RNA interference targeted to multiple P2X receptor subtypes attenuates zinc-induced calcium entry. Am J Physiol Cell Physiol 2005;289:C388-396.
23 Doctor RB, Matzakos T, McWilliams R, Johnson S, Feranchak AP, Fitz JG: Purinergic regulation of cholangiocyte secretion: Identification of a novel role for P2X receptors. Am J Physiol Gastrointest Liver Physiol 2005;288:G779-786.
24 Gum RJ, Wakefield B, Jarvis MF: P2X receptor antagonists for pain management: Examination of binding and physicochemical properties. Purinergic Signal 2012;8:41-56.
25 Virginio C, Robertson G, Surprenant A, North RA: Trinitrophenyl-substituted nucleotides are potent antagonists selective for P2X1, P2X3, and heteromeric P2X2/3 receptors. Mol Pharmacol 1998;53:969-973.
26 Jarvis MF, Khakh BS: ATP-gated P2X cation-channels. Neuropharmacology 2009;56:208-215.
27 Fisher R, Grützmann R, Blasco HPJ, Kalthof B, Gadea PC, Stelte-Ludwig B, Woltering E, Wutke M: Benzofuro-1,4-diazepin-2-one derivatives. 2005; Patent Number: EP1608659A1
28 Norenberg W, Sobottka H, Hempel C, Plotz T, Fischer W, Schmalzing G, Schaefer M: Positive allosteric modulation by ivermectin of human but not murine P2X7 receptors. Br J Pharmacol 2012;167:48-66.
29 Kwon HJ: Extracellular ATP signaling via P2X(4) receptor and cAMP/PKA signaling mediate ATP oscillations essential for prechondrogenic condensation. J Endocrinol 2012;214:337-348.
30 Wu T, Dai M, Shi XR, Jiang ZG, Nuttall AL: Functional expression of P2X4 receptor in capillary endothelial cells of the cochlear spiral ligament and its role in regulating the capillary diameter. Am J Physiol Heart Circ Physiol 2011;301:H69-78.
31 Casati A, Frascoli M, Traggiai E, Proietti M, Schenk U, Grassi F: Cell-autonomous regulation of hematopoietic stem cell cycling activity by ATP. Cell Death Differ 2011;18:396-404.
32 Hamill OP, Marty A, Neher E, Sakmann B, Sigworth FJ: Improved patch-clamp techniques for high-resolution current recording from cells and cell-free membrane patches. Pflugers Arch 1981;391:85-100.
33 He ML, Zemkova H, Koshimizu TA, Tomic M, Stojilkovic SS: Intracellular calcium measurements as a method in studies on activity of purinergic P2X receptor channels. Am J Physiol Cell Physiol 2003;285:C467-479.
34 Fischer W, Wirkner K, Weber M, Eberts C, Koles L, Reinhardt R, Franke H, Allgaier C, Gillen C, Illes P: Characterization of P2X3, P2Y1 and P2Y4 receptors in cultured HEK293-hP2X3 cells and their inhibition by ethanol and trichloroethanol. J Neurochem 2003;85:779-790.
35 Fischer W, Franke H, Groger-Arndt H, Illes P: Evidence for the existence of P2Y1,2,4 receptor subtypes in HEK-293 cells: Reactivation of P2Y1 receptors after repetitive agonist application. Naunyn Schmiedebergs Arch Pharmacol 2005;371:466-472.
36 Serrano A, Mo G, Grant R, Pare M, O'Donnell D, Yu XH, Tomaszewski MJ, Perkins MN, Seguela P, Cao CQ: Differential expression and pharmacology of native P2X receptors in rat and primate sensory neurons. J Neurosci 2012;32:11890-11896.
37 Nagata K, Imai T, Yamashita T, Tsuda M, Tozaki-Saitoh H, Inoue K: Antidepressants inhibit P2X4 receptor function: A possible involvement in neuropathic pain relief. Mol Pain 2009;5:20.
38 Khakh BS, Proctor WR, Dunwiddie TV, Labarca C, Lester HA: Allosteric control of gating and kinetics at P2X(4) receptor channels. J Neurosci 1999;19:7289-7299.
39 Asatryan L, Popova M, Perkins D, Trudell JR, Alkana RL, Davies DL: Ivermectin antagonizes ethanol inhibition in purinergic P24 receptors. J Pharmacol Exp Ther 2010;334:720-728.
40 Manohar M, Hirsh MI, Chen Y, Woehrle T, Karande AA, Junger WG: ATP release and autocrine signaling through P2X4 receptors regulate γδ T cell activation. J Leukoc Biol 2012;92:787-794.
41 Gong QJ, Li YY, Xin WJ, Zang Y, Ren WJ, Wei XH, Li YY, Zhang T, Liu XG: ATP induces long-term potentiation of c-fiber-evoked field potentials in spinal dorsal horn: The roles of P2X4 receptors and p38 MAPK in microglia. Glia 2009;57:583-591.
42 Li C, Peoples RW, Weight FF: Ethanol-induced inhibition of a neuronal P2X purinoceptor by an allosteric mechanism. Br J Pharmacol 1998;123:1-3.
43 Michel AD, Chambers LJ, Walter DS: Negative and positive allosteric modulators of the P2X(7) receptor. Br J Pharmacol 2008;153:737-750.